RESEARCH PAPER | Chemistry | Volume : 5 | Issue : 6 | June 2015 | ISSN - 2249-555X

Structural Studies and Morphology of Chemically Treated Sisal Fibre Aluminum Nitrate Composites

KEYWORDS: Al2O3, sintering method, calcinations, TEM and FTIR

Asif jehan

Motilal vigyan mahavidhalya Bhopal (M.P.) India

ABSTRACT *The current study shows the effect of chemical treatment on the structure and morphology of sisal fibre. In the present study sisal fibre is treated with aluminum nitrate salt. The treatment is done at 1000oC temperature using annealing method. X ray diffraction of the treated sisal fibre reveals the crystalline nature of the fibre. Change in morphology has been found in sisal fibre when subjected to Scanning Electron Microscopy.*

Introduction

Aluminum oxides are chemical compounds composed of aluminum and oxygen. All together, there are sixteen known aluminum oxides and oxyhydroxides. [1-2] Aluminum (III) oxide or aluminum oxide is the inorganic compound with the formula Al_2O_3. Powder metallurgy comprises a set of processes of forming having for common denominator a raw material in a powder form. The reduced aluminum powder is the most widely used material in powder metallurgy industry.$LiAlO_2$ has various crystalline structures such as α- $LiAlO_2$, β-$LiAlO_2$, γ-$LiAlO_2$, Layered $LiAlO_2$, Corrugated $LiAlO_2$, Goethite type $LiAlO_2$ etc. The crystalline structure of $LiAlO_2$ depends mainly on the preparation methods. Many researches prepared $LiAlO_2$ with different structures. α-$LiAlO_2$ with Fm-3m space group by using solid state reaction and α-$LiAlO_2$ with Fm3m space group by hydrothermal synthesis [3-5].

The geo polymers were made using metakaolin, calcium hydroxide, sodium hydroxide, sodium silicate and water. The geo polymers contained two or three phases, depending on whether or not calcium hydroxide was used. For geo polymers with no calcium hydroxide, the samples contained two phases: unreacted metakaolin and geo polymer gel. To ensure geo polymer gel was forming and to monitor the amount of the geo polymer gel, hydrochloric (HCl) acid extractions were performed. For geo polymers with calcium hydroxide, samples contained three phases: unreacted metakaolin, geo polymer gel and calcium silicate hydrate with aluminum substitution (CASH). In conjunction with the HCl extraction, salicylic acid/methanol (SAM) extractions were performed to verify the presence and amounts for each phase. X-ray diffraction (XRD) was used to identify crystalline phases as well as monitor the changes in the amorphous peak from metakaolin to geo polymer. XRD analysis showed that the geo polymers with varying Si/Al ratios produced the same pattern. The patterns with calcium hydroxide in the geo polymer produced an amorphous peak that was narrower and centered at higher 2Θ value than the geo polymers with no calcium hydroxide. The patterns also confirmed the presence of calcium silicate hydrate in XRD patterns. Both Si and Al [6] magic angle spinning nuclear magnetic resonance (MAS-NMR) were used to quantitatively observe the individual silicon and aluminum structures in the different phases in the geo polymer. From Si NMR analysis, the composition and amount of the different phases in the geo polymer could be determined. Increasing the Si/Al ratio caused a decrease in Si-O-Al bonds and an increase in Si-O-Si bonds in the geo polymer gels, which caused the compressive strength in the geo polymer to increase. The Si [7] NMR analysis showed that geo polymers with calcium hydroxide produced calcium silicate hydrate that had cross-linking tetrahedral with alumina substitution in bridging tetrahedral sites. The increasing amount of calcium hydroxide increased the amount of CASH and decreased the amount of the geo polymer gel. Increasing calcium hydroxide caused the Si/Al ratio of the geo polymer gel to decrease. The combination of geo polymer gel and CASH increased the strength of the geo polymer gel [8].

Silicon dioxide (SiO_2) is the most commonly used gate dielectric in metal-oxide-semiconductor (MOS) devices due to its chemical and thermal stability on Si substrates [9]. The SiO_2 thickness has been decreased significantly in the development of high-speed advanced semiconductor devices [10-11]. However, the gate oxide thickness can-not be reduced below 2 nm because of reliability problems associated with conventional SiO_2 and high leakage currents caused by direct tunneling across the gate dielectric film [12-13]. Based on these restrictions, high dielectric-constant materials are required as alternative gate insulators in advanced MOS devices [14-15]. Compared to SiO_2 films, high dielectric-constant films can provide larger physical thicknesses and significant reductions in leakage currents for the same equivalent oxide thickness (EOT) [16-17]. Among the high-dielectric-constant materials, HfO_2,Al_2O_3, ZrO_2, and Ta_2O_5 have been extensively studied to solve the excessively high leakage-current concern for future advanced high performance devices [18-19]. Al_2O_3 and HfO_2 are considered to be the most attractive materials among the high dielectric materials. Also, Al_2O_3has been studied in ultra-large-scale integrated devices because it remains amorphous even after annealing at temperatures as high as 1000°C [20]. In addition, Al_2O_3 exhibits a large band gap (~8.8 eV), a high field strength, a excellent thermal stability, and large band offsets [21].

In the present study the main objective was to find effect of chemical treatment of sisal fibre and see changes on the structure and morphology of fibre. It desired result is obtained the use the chemically treated sisal fibre.

Process

Aluminum Nitrate ($Al(NO_3)_3$. $9H_2O$) and ammonium chloride (NH_4Cl) was taken in the ratio 10:4 in 500 *ml* of distilled water. The mixture was stirred till a homogenous solution was obtained. In this mixture 10g of processed sisal fiber was

Volume : 5 | Issue : 6 | June 2015 | ISSN - 2249-555X

added and then 1:1 solution of NH_4OH (liquid ammonia) was added to it and left the solution for one hour. Again the mixture thus obtained was dried and then annealed in muffle furnace at 1000°C and kept it at that temperature for different time duration sample 1 (SP1) for 15 min, sample 2 (SP2) for 30 min and sample 3 (SP3) for 45 min.

The reaction may take place in this way

$2Al(NO_3)_3.9H_2O + 3NH_4Cl + 3NH_4OH + Fiber \rightarrow$ **Al_2O_3: fiber** (Aluminum oxide: fiber) + $6NH_4NO_3$ + 3HOCl + $18H_2O$

When aluminum nitrate reacts with ammonium chloride and ammonium hydroxide along with sisal fiber at 1000°C aluminum oxide is formed which is confirmed through XRD analysis and other by products like $6NH_4NO_3$ Ammonium nitrate and HOCl (hypoclorous acid) decomposed at such high temperature and only aluminum oxide is left .

Result and discussion

TEM

Fig 7 (a) (b) and (c) for SP1, SP2 & SP3 respectively shows the non linear and non uniform dispersed aluminum oxide particles of 110.57nm and the agglomerated fiber containing 284.63-156.92nm size particles of aluminum oxide. The samples appear highly strained as seen in fig 7 (a) (b) and (c). The presence of dislocation loops is clearly seen. It is possible that the strain present in the sintered samples has a direct effect on the dielectric loss. The TEM micrographs show the heterogeneous microstructure aluminum oxides. A heterogeneous distribution of the individual phases is observed in all heterogeneous systems. On the other hand, in the aluminum oxide samples the particles possess needles like morphology with non-uniform sizes in a range from 110.57nm to 284.63-156.92nm. These needles are less in numbers but large in size. The TEM investigations of the aluminum oxide composite samples show heterogeneous distribution with aluminum oxide needle like structure of about 30nm sizes. The diffraction pattern shows a higher grade of crystalline for the high aluminum oxide containing sample. The first fig shows the magnification 40000 which shows total palate of size of 110.57nm, second fig shows with the magnification of 60000 which is clearly shows the fibrous portion of the palate 284.63nm and third fig shows the magnification of 12000 which again shows the fibrous portion of the palate 156.92nm.

Table 1

Name	Symbol	Classification	A	B
Cellulose	$C_6H_{10}O_5$	C-H Deprotonation	C	H
Hemicelluloses	$C_5H_{10}O_5$	C-H Deprotonation	C	H
Lignin	$C_{13}H_{34}O_{11}$	C-H Deprotonation	C	H

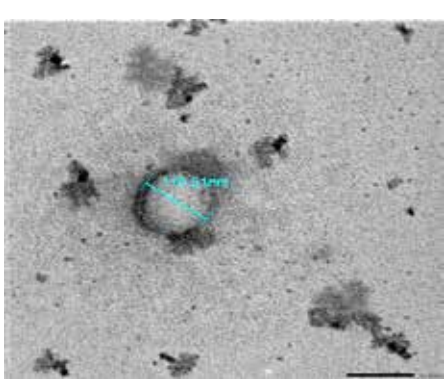

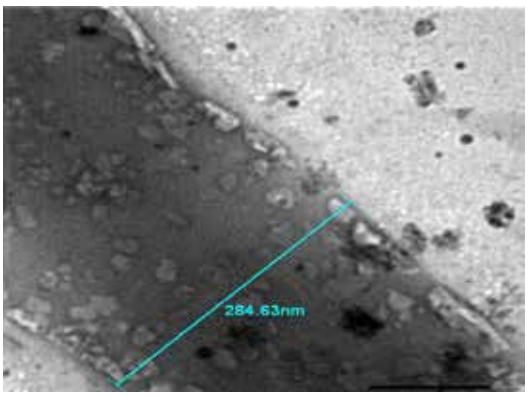

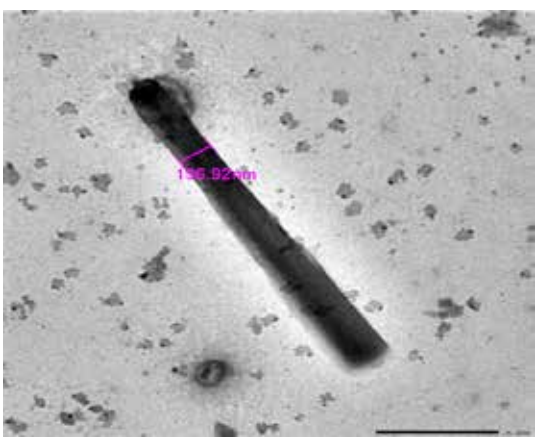

Fig (c)

Fig 4. (a) (b) and (c) TEM of Al_2O_3 to find the structure and composition of the sample prepared in our studies.

The TEM graphs show the highly homogeneous microstructure if Al_2O_3 samples the aluminum nitrate and ammonium chloride (10:4) one has still amorphous particles. The TEM investigations of the Al_2O_3 composite samples show heterogeneous distribution with needle like structure. Among the sisal fiber doped aluminum samples with the composition has a longer amount of pores in the microspores region. Hence the pores size can be adjusted by the composition according to needs of the applications TEM observations confirmed the homogeneity of the microstructure. The morphology of the composites consists of aluminum oxide needles with high aspect ratio. It is possible to synthesize materials with different porosity features and surface morphology, which result in different applications by changing the ration of individual components in oxide system [24].

FTIR

The formation of α-Al_2O_3 was approved by FTIR spectrum in figures showed that α-Al_2O_3 is known to have spinal structures which exist over a range of hydrogen content captured by the empirical formula $H_{3m}Al_{2-m}O_3$. It is clear that broad absorption bands appear at 3500-500cm^{-1} respectively, which is attributed to the stretching vibration of hydroxyl groups. The peaks at 3127.07, 1399.42 and 584.57 cm^{-1} correspond to the vibration of carboxylic acid groups. The IR transmission spectra of sisal fiber composite shown in fig from fig 8, 9 & 10 for SP1, SP2 & SP3 respectively were recorded in the range 3700-3400 cm^{-1}. The wave number of fig 8 (SP1) 3127.0691,

Volume : 5 | Issue : 6 | June 2015 | ISSN - 2249-555X

2358.4974, 1641.0773, 1399.4211 and 584.5742cm^{-1} shows the width 1471.2957, 1716.5060, 82.7603, 40.8444 and 378.2537cm^{-1} of IR spectra respectively.

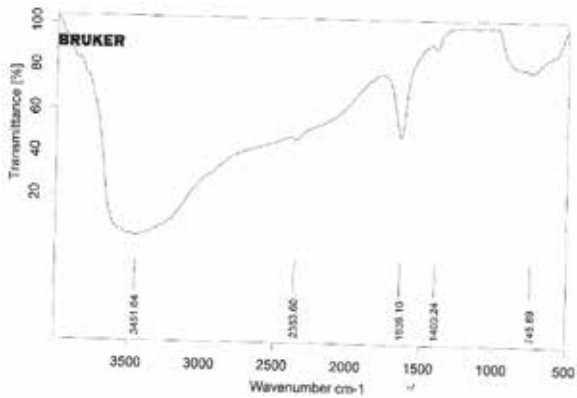

Fig. 6 Intensity of Transmittance versus wave number (courtesy SIRT-F Bhopal)

The prepared sample was free from visible inhomogeneities like cracks or bubbles. Decrease with a shifting of meta-center towards slightly higher wave number. For further increase of Al_2O_3 the intensity of this band is continued to decrease where the first group of bands is also observed to decrease [25]. The peaks at 3447.86, 1639.35 and 586.54 cm^{-1} correspond to the vibration of carboxylic acid group. The wave number of fig 9 (SP2) 3447.86, 2360.13, 2072.60, 1639.35, 1397.30, 642.20 and 586.54 cm^{-1} shows the width 445.6188, 60.6905, 203.3672, 82.8672, 44.0294, 92.4690 and 294.6694 cm^{-1} of IR spectra respectively.

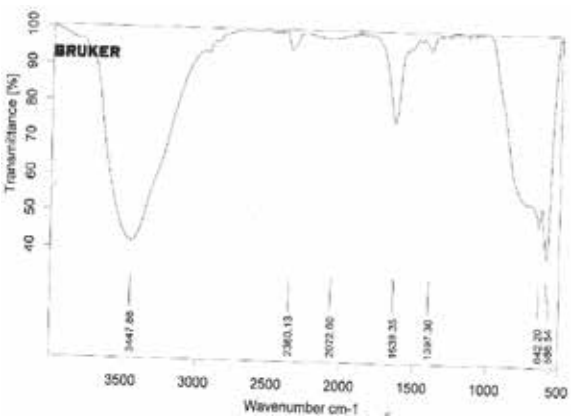

Fig. 7 Intensity of Transmittance versus wave number another sample (courtesy SIRT-F Bhopal).

The peaks at 3450.73, 1638.44 and 589.85 cm^{-1} correspond to the vibration of carboxylic acid group. The wave number of fig 10 (SP3) 3450.73, 2360.94, 1638.44, 74004 and 589.85 cm^{-1} shows the width 558.7216, 54.5087, 79.0997, 366.1014 and 46694.4103 cm^{-1} of IR spectra respectively. The prepared sample was free from visible inhomogeneities like cracks or bubbles. Decrease with a shifting of meta-center towards slightly higher wave number. For further increase of Al_2O_3 the intensity of this band is continued to decrease where the first group of bands is also observed to decrease [25].

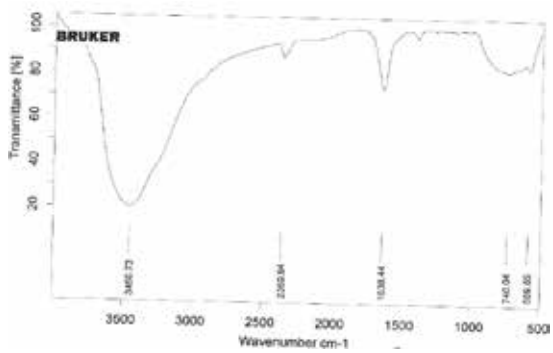

Fig.8 has several valleys imitating influence of dopants. The prominent valley at 3437 cm^{-1} is interesting (courtesy SIRT-F Bhopal).

The stronger broadening bands 3500-1000 cm^{-1}for SP1, 3400-900 cm^{-1} for SP2 and 3300-800 cm^{-1}for SP3 occurs due to the hydrogen bond between the various hydroxyl groups in the product. The stronger broadening bands 3700-3400 cm^{-1} for SP1, SP2 & SP3 correspond to Al-O vibration existed under the temperature of 1000°C at 15, 30 and 45 min for SP1, SP2 and SP3 respectively. In agreement with other works it is resulted that the main factor in obtaining of different aluminum oxide phases is the calcinations temperature at 1000°C leads to form the α-Al_2O_3 [26].

Conclusion

The effect of chemical homogeneity, fine structure, particle size and shape of the aluminum samples are understood to affect the properties of its TEM and FTIR behavior. The presence of moisture, cellulose, hemicelluloses, lignin and pectin also contribute towards changes in composites properties. In this agreement with other works, it is resulted that the main factor in obtaining of alumina is the calcinations temperature on different time durations.

REFERENCE

1. Cornell, RM; Schwertmann, U (2003). The aluminum oxides: structure, properties, reactions, occurrences and uses. Wiley VCH. ISBN 3-527-30274-3. | | 2. Bienvenu, Y., Rodrigues, S. Manufacture of Metal Powders from Pulverulent Waste, ENSMP, Centre des matériaux, CNRS UMR 7633, France (2007). | | 3. Lee, Y.S.; Sato, S.; Tabuchi, M.; Yoon, C.S.; Sun, Y.K.; Kobayakawa, K.; Sato, Y. lectrochem. Commun. 2003, 5, 549. DOI: 10.1016/S1388-2481(03)00118-8 | 4. Masaaki Hirayama.; Hiroki Tomita.; Kei Kubota.; Ryoji Kanno.; J. Power Sources 2011, 196, 809. DOI: 10.1016/j.jpowsour.2010.10.009 | | 5. Galakhov, V.R.; Kurmaev, E.Z.; Uhlenbrock, S. Solid State Commun. 1995, 95, 347. DOI: 10.1016/0038-1098(95)00279-0 | | 6. Struble, L. The effects of water on maleic and salicylic acid extraction. Cem. and Con. Res.Vol. 15. 1985. | | 7. Duxson P, Provis JL, Lukey GC, Separovic F. and van Deventer JSJ. Si NMR Study of Structural Ordering Aluminosilicate Geopolymer Gels. Langmuir2005(21) 3028-3036. | | 8. UNDERSTANDING EFFECTS OF SILICON/ALUMINUM RATIO AND CALCIUM HYDROXIDE ON CHEMICAL COMPOSITION, NANOSTRUCTURE AND COMPRESSIVE STRENGTH FOR METAKAOLIN GEOPOLYMERS BY ERIC HEYSUNG KIM THESIS Submitted in partial fulfillment of the requirements for the degree of Master of Science in Civil Engineering in the Graduate College of the University of Illinois at Urbana-Champaign, 2012 | | 9. A. Khandelwal, H. Niimi, G. Lucovsky and H. Henry Lamb, J. Vac. Sci. Technol.\0, 1989 (2002). | | 10. P. A. Packan, Science285, 2079 (1999). | | 11. M. Schulz, Nature399, 729 (1999). | | 12. H. Fukuda, M. Yasuda and T. Iwabuchi, Appl. Phys.Lett.61, 693 (1992). | | 13. M. Copel, M. A. Gribelyuk and E. P. Gusev, Appl. Phys.Lett.76, 436 (2000). | | 14. A. I. Kingon, J. P. Maria and S. K. Streiffer, Nature406,1032 (2000). | | 15. C. Chaneliere, J. L. Autran, R. A. B. Devine and B.Balland, Mater. Sci. Eng. R22, 269 (1998). | | 16. G. D. Wilk, R. M. Wallace and J. M. Anthony, J. Appl.Phys.87, 484 (2000). | | 17. Y. Kim, J. Koo, J. Han, S. Choi, H. Jeon and C. Park,J. Appl. Phys.92, 5443 (2002). | | 18. S. Gopalan, K. Onishi, R. Nieh, C. S. Kang, R. Choi, H.J. Cho, S. Krishna and J. C. Lee, Appl. Phys. Lett.80,4416 (2002). | | 19. J. Lee, J. Koo, H. S. Sim and H. Jeon, J. Korean Phys.Soc.44, 915 (2004). | | 20. A. Chin, C. C. Liao, C. H. Lu, W. J. Chen and C. Tsai,Symp. VLSI Tech. Dig. 135 (1999). | | 21. E. P. Gusev, M. Copel, E. Cartier, I. J. R. Baumvol, C.Krug and M. A. Gribelyuk, Appl. Phys. Lett.76, 176(2000). | | 22. S yusub, Gsahaya baskaranet al Indian journal of pure &applied physics Vol. 49 May 2011. Pp 315-322. | | 23. Schmittle, M.; Burghart, A. Angew. Chem. int. Ed. EEngl.1997, 36, 2550. | | 24. W. Wunderlich, P. Padmaja, K.G.K. Warrier TEM characterization of sol-gel-processed alumina–silica and alumina–titania nano-hybrid oxide catalysts Journal of the European Ceramic Society 24 (2004) 313–317 | | 25. S yusub, Gsahaya baskaranet al Indian journal of pure &applied physics Vol. 49 May 2011. Pp 315-322. | | 26. Seyed Ali Hosseini, Aligholi Niaei, Dariush Salari Production of γ-Al2O3from Kaolin Open Journal of Physical Chemistry, 2011, 1, 23-27 doi:10.4236/ojpc.2011.12004 Published Online August 2011 |